Magnetic static and scaling properties of the weak random-axis magnet $(Dy_xY_{1-x})Al_2$

P.M. Gehring* and M.B. Salamon
Department of Physics and Materials Research Laboratory, University of Illinois at Urbana-Champaign, 1110 West Green Street, Urbana, Illinois 61801

A. del Moral and J.I. Arnaudas
Magnetismo de Solidos, Departamento de Fisica de la Materia Condensada, Instituto de Ciencia de Materiales de Aragón Universidad de Zaragoza y Consejo Superior de Investigaciones Cientificas, 50009 Zaragoza, Spain
(Received 18 October 1989)

The effects of a random component of the magnetocrystalline anisotropy on the magnetic properties and critical behavior of polycrystalline $DyAl_2$ have been investigated using dc-magnetic measurements. Random magnetic anisotropy (RMA) is produced by site-diluting ferromagnetic $DyAl_2$ with the non-magnetic, isomorphic intermetallic YAl_2. Dilution distorts the cubic Laves phase unit cell because of a slight lattice mismatch thereby lowering the local crystal symmetry in a random fashion. Additional contributions to the RMA come from spin-orbit scattering by the conduction electrons. Hysteresis loops display little remanence and very small coercive fields, suggesting a weak RMA. This is consistent with estimates of the RMA strength D obtained using an approach of Chudnovsky *et al.* The magnetization at high temperatures ($T > 4T_c$) is well described by a Curie-Weiss law. The paramagnetic Curie temperatures are positive, implying an average ferromagnetic exchange coupling between Dy ions, and increase with x. The paramagnetic moment shows no evidence of quenching across the series, thus confirming the well localized nature of the $4f$ electronic orbitals. Low-field thermal scans of the bulk dc magnetization show no sign of a spontaneous moment for Dy concentrations $0.10 \leq x \leq 0.90$, yet a sharp increase in the magnetization occurs at a temperature T_c that increases with x. A ferromagnetic scaling analysis applied to the line of transitions at T_c results in a surprisingly good collapse of the magnetization data. By extending prior theoretical work of Aharony and Pytte, a direct connection can be made between pure and RMA exponents which gives remarkable agreement with the experimental values.

I. INTRODUCTION

Magnetic dilution has long been used to probe the nature and strength of interactions between magnetic moments as well as to produce novel magnetic phases and ordering phenomena. Of particular interest are the effects of site dilution, where a magnetic species is replaced at random by a nonmagnetic counterpart at well-defined crystallographic sites. The composition of the resulting compound is commonly referenced by its relative concentration x, which gauges the concentration of the magnetic species relative to that of the nonmagnetic species. Hence, the pure ferromagnetic compound has $x = 1$. Such systems are said to possess "quenched" or static disorder because the impurities are rigidly frozen into fixed positions and are not free to diffuse at the temperatures under study. This is in constrast to systems with "unquenched" or "annealed" disorder where the impurities are free to reach thermal equilibrium with other degrees of freedom.[1]

The random-axis magnet[2,3] is an example of a system possessing quenched magnetic disorder. This system is one for which all macroscopic directions are equally "hard" magnetically in that it requires energy to align the magnetization along any single direction. Yet, because the local magnetic anisotropy varies from site to site, there is a broad spatial distribution of local "easy" axes of magnetization. Because of their random magnetic anisotropy (RMA), random-axis magnets are also referred to as RMA magnets.

In recent years, a number of studies have addressed questions concerning long-range magnetic order (LRMO) and critical phenomena in systems with a random spin anisotropy, and they represent the primary motivation for this paper.[2-7] Nevertheless, the true ground state spin configuration for the RMA magnet at low temperatures is still not understood, nor is the nature of the transition from the paramagnetic to low temperature phase. In this paper, it will be demonstrated that the properties of the Laves-phase intermetallic $(Dy_xY_{1-x})Al_2$ are best understood in the context of the weak RMA model. Among these properties are the absence of a spontaneous magnetization, changes in the critical exponents, and a slow approach to saturation.

The next section briefly reviews theoretical approaches

to the random magnetic anisotropy problem. Experimental results that bear on current physical understanding are also discussed. Because the original physical context for random-axis magnets was in amorphous systems, they necessarily dominate the subsequent discussion. Following this section, the growth and characterization of the $(Dy_xY_{1-x})Al_2$ compounds are discussed briefly in Sec. III. The RMA strength and characteristics of $(Dy_xY_{1-x})Al_2$ are examined in Sec. IV, with the magnetization data and scaling analysis presented in Sec. V. Results and conclusions are summarized in Sec. VI.

II. THEORETICAL AND EXPERIMENTAL BACKGROUND

A. The RMA model Hamiltonian

In 1972, Rhyne *et al.* presented evidence for the first direct observation of an amorphous spin-polarization distribution obtained from neutron scattering experiments on sputtered samples of (amorphous) a-$TbFe_2$.[8] Concurrent bulk magnetization measurements of the same material surprisingly indicated the presence of a macroscopic spontaneous magnetization, the definition of ferromagnetic (FM) ordering. However, the Curie temperature T_c and saturation magnetization M_s of a-$TbFe_2$ are about half as large as that of the corresponding crystalline phase. The results of Rhyne *et al.* are particularly interesting in that they allowed the first direct comparison between the magnetic properties of the crystalline and amorphous phases of materials whose percentage atomic composition ($TbFe_2$) are identical.

Stimulated by the effects of a random spin distribution on the basic magnetic properties of a-$TbFe_2$, Harris, Plischke, and Zuckermann[4] (HPZ) proposed a magnetic model to account for these experimental observations. They were cognizant of the strong magnetocrystalline anisotropy present in $TbFe_2$ and other compounds containing heavy, non-S-state, rare-earth ions that are predominantly single-ion in nature.[9] Since single-ion anisotropy is founded in the strong coupling between the aspherical 4f electron clouds of the rare-earth ions and the crystalline electric field, HPZ viewed the randomness in the local magnetic anisotropy as the most important characteristic of these amorphous alloys. This randomness, which produces highly irregular local electrostatic fields, is a direct consequence of the topological disorder inherent to the amorphous state. Consequently, HPZ formulated a Hamiltonian that included a sum over the local single-ion anisotropy fields.

The HPZ Hamiltonian is a Heisenberg model where all spins have identical magnitude, but where each spin is coupled to a local electrostatic field, analogous to the usual crystalline electric field (CEF), which varies randomly from site to site. Their Hamiltonian has the basic form[4]

$$\mathcal{H} = \sum_i V_i - \tfrac{1}{2}\mathcal{J}\sum_{i,\delta} \mathbf{J}(i)\cdot\mathbf{J}(i+\delta)\,, \tag{1}$$

where V_i is the local single-ion anisotropy field at site i, $\mathcal{J}$ is the nearest-neighbor Heisenberg exchange coupling constant, and $\mathbf{J}(i)$ represents the angular momentum operator for the magnetic ion on site i. This form does not take into account the distribution of values for the Heisenberg exchange coupling constant $\Delta\mathcal{J}$ which occurs due to the structural disorder of amorphous alloys. In principle, this should be included, although it is argued that the effects of RMA on the magnetic properties of the heavy rare-earth alloys such as TbAg should dominate over those based on the exchange interaction.[10] Experimentally, however, this argument seems to hold only in the limit of very high fields in excess of 100 kOe, where a mean-field analysis of the HPZ Hamiltonian yields good fits to the field dependence of the magnetization of both TbAg and DyAg alloys.[11]

The calculation of the explicit form for the anisotropy field V_i in the HPZ Hamiltonian is couched in the language of conventional crystal field theory. After some simplifications and approximations, the Hamiltonian can be reduced to[10]

$$\mathcal{H}_{\rm RMA} = -D\sum_i (J_{z_i})^2\,, \tag{2}$$

where $D > 0$ is a measure of the random uniaxial anisotropy strength. Most theoretical work is based on this Hamiltonian. Thus, the final form for the total Hamiltonian can be written as

$$\mathcal{H} = -\mathcal{J}\sum_{i,j}\mathbf{J}_i\cdot\mathbf{J}_j - D\sum_i(\hat{\mathbf{n}}_i\cdot\mathbf{J}_i)^2 - g\mu_B\sum_i \mathbf{H}\cdot\mathbf{J}_i\,,$$

where $\hat{\mathbf{n}}_i$ is a unit vector that points in the direction of the local random anisotropy. Since the axes z_i are randomly distributed from site to site in amorphous systems, $\hat{\mathbf{n}}_i$ possesses a spherical distribution. It is important, however, to note that in a crystalline system such as $(Dy_xY_{1-x})Al_2$, $\hat{\mathbf{n}}_i$ will be limited to a finite number of directions.

B. Equation of state approach

A mean-field treatment of the HPZ Hamiltonian yields a ferromagnetic phase when $\mathcal{J} > 0$.[4] Indeed, until 1980, a variety of amorphous rare-earth alloys had been studied and were believed to possess long-range ferromagnetic or ferrimagnetic order below a finite transition temperature.[12,13] This view persisted even after theoretical papers by Imry and Ma[5] and Pelcovits *et al.*[14] cast serious doubts on the mean-field predictions of HPZ. However, in 1980 a seminal paper by Aharony and Pytte[2] (AP) focused attention on how experimental data should be analyzed, calling into question the methods of analysis used in these experimental studies. Their results reconciled the apparent discrepancy between those theories which predicted the absence of LRMO in systems with quenched random interactions and experimental Arrott plots which seemed to show the presence of a spontaneous moment.

Aharony and Pytte calculated the magnetic equation

of state for both RMA and random-field (RF) systems and found no LRMO in either case. The RMA equation of state has the form

$$\frac{H}{M} = t + M^2 + a_A \left(\frac{n-1}{n(n+2)}\right)\left(\frac{D}{\mathcal{J}}\right)^2 M^2 \left(\frac{H}{M}\right)^{-\epsilon/2} , \tag{4}$$

where a_A is a constant of order unity for $d = 3$, n is the number of spin components, $\epsilon = 4 - d$, and t the usual reduced temperature. The resulting Arrott plots make apparent the destruction of LRMO as none of the isotherms intercept the M^2 axis at any finite value. From their conclusions, it was clear that extrapolating Arrott plot isotherms from high fields towards $H = 0$ would result in artificially lower estimates for T_c and would yield false indications of finite spontaneous moments.

The most spectacular of AP's results was the prediction that all isotherms reach the origin below T_c. This means that, even though there is no LRMO, the zero field or initial susceptibility $\chi_0 \to \infty$ as $T \to T_c^+$. No such behavior was found in the random field case. AP characterized their infinite susceptibility phase through the field dependence of the magnetization. Ignoring critical fluctuation effects, they found that for low field strengths

$$M \sim H^{1/\delta}, \text{ where } \begin{cases} \delta = \dfrac{10-d}{6-d} & \text{for } T = T_c \\ \delta = \dfrac{8-d}{4-d} & \text{for } T < T_c \end{cases} . \tag{5}$$

In three-dimensional systems, these exponents reduce to $\frac{7}{3}$ and 5, respectively. The magnetic susceptibility is then

$$\chi \equiv \frac{\partial M}{\partial H} \sim H^{-x}, \text{ where } \begin{cases} x = \frac{4}{7} & \text{for } T = T_c \\ x = \frac{4}{5} & \text{for } T < T_c \end{cases} . \tag{6}$$

Clearly $\chi \to \infty$ as $H \to 0$, provided $T \leq T_c$.

Although extensive experimental tests of the AP conjecture failed to yield any definitive evidence for the infinite susceptibility phase,[15] various other aspects of their theory were verified, namely the lack of a spontaneous moment and a change in the value of δ near T_c. Several systems, covering a range of RMA strengths from $0.001 \leq D/\mathcal{J} \leq 2$, were used in these tests. There was no spontaneous magnetization in the large RMA system, but the initial susceptibility remained finite at all temperatures. On the other hand, the magnetic susceptibility in the weak RMA system actually did diverge, however a small moment was observed as well. This prompted the belief that the AP magnetic equation of state was valid only in the limit where $D \ll \mathcal{J}$. Aharony and Pytte stressed this themselves and said that their calculations had been carried out only to lowest order in $(D/\mathcal{J})^2$. In systems with larger RMA strengths, higher order terms would have to be included. In a later publication,[6] Aharony and Pytte suggested the effects of higher-order terms would limit the susceptibility to a value $\propto (\mathcal{J}/D)^4$. This has since been verified by Barbara *et al.*[16] in *a*-$Dy_xGd_{1-x}Ni$, but only when $\mathcal{J}/D$ is less than 3. For weaker RMA, the $T = 0$ susceptibility actually seems to level off, showing a markedly weaker dependence on $\mathcal{J}/D$.

In 1985, Goldschmidt and Aharony[7] (GA) considered the effects of a coherent anisotropy in the limit $N \to \infty$. They demonstrated that LRMO is stabilized by a second-order phase transition in systems that possess a sufficient degree of coherent uniaxial anisotropy to break the rotational invariance of the RMA. For systems with higher order coherent anisotropies, e.g., cubic or hexagonal, the transition is first order. This has the effect of masking the "pure" RMA properties detailed above inasmuch as it is impossible to subtract out the effects of a parasitic coherent anisotropy from the experimental data. However, an especially interesting result occurs at a threshold uniaxial strength g_c, which marks the phase boundary between the ferromagnetic and spin-glass phases. At this point the AP infinite susceptibility phase is recovered, even after *all* orders in $D/\mathcal{J}$ have been taken into account. Still, there is no true theoretical consensus concerning the nature of the low-temperature phase in RMA systems. Indeed, Fisher[17] argues that the spin-glass phase is unstable to leading order in $1/N$, leaving this issue an open question.

C. Perturbation approach: The weak RMA limit

A more phenomenological approach was reported in 1986 by Chudnovsky, Saslow, and Serota[3] (CSS), who examined the additional effects induced in RMA systems through application of a finite field that, until then, had received scant attention. The study of CSS, a perturbative approach which emphasizes the weak RMA limit, is based on the macroscopic energy density

$$\varepsilon = \tfrac{1}{2}\alpha(\nabla_i M_\mu)(\nabla_i M_\mu) - \tfrac{1}{2}\beta_r(\mathbf{M}\cdot\hat{\mathbf{n}}_r)^2 - \mathbf{M}\cdot\mathbf{H} , \tag{7}$$

where $\alpha \propto \mathcal{J}a^2$. $\mathcal{J}$ is the average exchange coupling between spins, a is an average interatomic spacing, and $\beta_r \propto D$ is the average RMA anisotropy strength. The magnetization $\mathbf{M}$ is assumed to be of a fixed length M_0, determined by the temperature T and the short-range exchange constants. The unit vector $\hat{\mathbf{n}}_r$ plays the same role as the unit vector in the HPZ Hamiltonian discussed earlier. Following their notation, they define three characteristic magnetic fields through the relations:

$$H_{ex} \equiv \alpha M_0 / R_a^2 , \tag{8}$$

$$H_r \equiv \beta_r M_0 , \tag{9}$$

$$H_c \equiv \beta_c M_0 , \tag{10}$$

where $\beta_c \propto D_c$ is the coherent anisotropy strength, and R_a is the length, measured in units of a, over which the local RMA axes are correlated. In amorphous alloys this length is assumed to be only a few lattice spacings, but

in polycrystals it is expected that $R_a \gg a$.[3]

In the strong anisotropy limit ($H_r > H_{ex}$), each spin is forced to point very nearly along the local easy axis of magnetization, and the aspects of ferromagnetic long-range order are essentially lost. An "arrow representation" of the spin structure is the same as that for a spin glass where the spins are frozen and randomly oriented in space such that there is no net moment. The magnetic susceptibility χ in this case is of order M_0/H_r, which is very small, and a large field is required to rotate the spins into a partial alignment within a hemisphere defined by the direction of the applied field. Strong coercivity and hysteretic behavior are observed in this limit.

The situation is drastically different when the RMA is weak compared to the exchange interaction ($H_r < H_{ex}$). Not surprisingly, several features exhibited by the system are strongly reminiscent of ferromagnetism. These include a large magnetic susceptibility, a large but finite ferromagnetic-like correlation length ξ over which the spins retain a local ferromagnetic order, and an ability to form domains. CSS identify three field-dependent regimes for weak RMA systems, determined by the strength of the applied field H relative to that of a characteristic field H_s defined by

$$H_s \equiv \left(\frac{H_r^4}{H_{ex}^3}\right) . \tag{11}$$

Following the nomenclature of CSS, the three classes of ordering are given.

1. The correlated spin glass (CSG)

When $H = 0$, the spins are spatially disordered and no spontaneous magnetization exists. The spin-spin correlations decay exponentially across the system with a correlation length ξ given by

$$\xi \sim \left(\frac{H_{ex}}{H_r}\right)^2 R_a , \tag{12}$$

so that over a length ξ, the weak RMA system possesses a local ferromagnetic order. On a large scale it has an arrow representation of a spin glass. There are no sharp domain walls between the ferromagnetically ordered regions as in a normal ferromagnet; instead, the width of the domain walls is comparable to that of the ordered regions, and the local magnetization undergoes continuous rotations over the entire length of the sample. In the presence of small fields $H < H_s$, the CSG remains. Unlike the strong RMA system, however, the CSG is easily magnetized, having a magnetic susceptibility which is quite large:

$$\chi_{CSG} = \left(\frac{15}{4}\right)^3 \frac{M_0}{2H_s} = \frac{1}{2\beta_r}\left(\frac{15}{4}\frac{H_{ex}}{H_r}\right)^3 \quad (n = 3,\ d = 3) . \tag{13}$$

2. The ferromagnet with wandering axis (FWA)

When $H \geq H_s$, the system is significantly polarized due to the combined effects of the applied field and the exchange interaction energy. This results in an almost collinear spin structure in which the spins are tipped from the applied field direction by an angle θ. The local RMA prevents complete alignment of the spins with **H** and causes the spin axes to wander with respect to **H**, hence the name ferromagnet with wandering axis.

Analytical results are much more easily obtained for the FWA state than for the CSG state because the nearly collinear structure is markedly less complex than the disordered, random spin structure of the CSG. For sufficiently large fields, the angle θ is small, allowing a perturbative treatment of the FWA regime. Using quantitative response function arguments, CSS were able to derive the field dependence of the FWA's approach to saturation:

$$\frac{\Delta M}{M_s} \equiv \frac{M_s - M}{M_s} = \frac{1}{15}\left(\frac{H_s}{H}\right)^{1/2} , \tag{14}$$

where M_s is the saturation magnetization. This form has been used with success by Sellmyer *et al.*[18] in characterizing the field dependence of the magnetization of a - $Gd_{72}Fe_{10}Ga_{18}$ at 4.2 K over a range of applied fields from 1 kOe $\leq H \leq$ 80 kOe. From their fit they obtained a value of 182 Oe for H_s. Thus the requirement that $H \geq H_s$ is certainly satisfied.

3. The large-field regime

This case is almost identical to that of the FWA except the spins now lie even more closely along the direction of **H**. The approach to saturation is more pronounced and obeys

$$\frac{\Delta M}{M_s} = \frac{1}{15}\left(\frac{H_r}{H + H_{ex}}\right)^2 , \tag{15}$$

which is valid for fields $H > H_{ex}$.

D. Experimental background

Although most experimental work on RMA systems has centered on the study of strong anisotropy, some studies have been performed in the weak RMA limit. These weak RMA systems are generally based on the S-state rare-earth ion Gd, as in a-GdAg, which was used in the study by von Molnar *et al.*[15] Its initial magnetic susceptibility χ_0 diverges at a finite temperature, but a small spontaneous moment appears as well. Other Gd-based alloys have been studied by Sellmyer *et al.*[18] These include the GdLaGB glasses, where G = Ga or Co. Zero-field ac-susceptibility measurements suggest these amorphous alloys undergo a ferromagnetic to spin-glass phase transition as the temperature is decreased. In addition, a scaling analysis was performed which gave good results for both the transitions, i.e., PM-FM and FM-SG. However, these compounds showed no signs of a spontaneous

moment, and their magnetic behavior was completely reversible above the spin-glass transition. Moreover, the approach to saturation was well described by that for the FWA, suggesting that the CSG picture might be more appropriate. Sellmyer *et al.* tried to reconcile the two observations, suggesting that in the presence of an applied field the CSG phase might revert to a FM state with appropriate critical exponents.

III. THE $(Dy_xY_{1-x})Al_2$ SYSTEM

A. The intermetallics $DyAl_2$ and YAl_2

$DyAl_2$ has been intensely studied in part due to the success of the RKKY model in describing many of its magnetic properties, such as the dependence of the Curie temperature on the interatomic ionic spacing.[19] Pure $DyAl_2$ and YAl_2 are intermetallic compounds that crystallize in the cubic-Laves phase[20] $C15$ ($Fd3m$) structure, isomorphic to that of $MgCu_2$. The rare-earth sites form a diamond lattice with each site having four nearest-neighbor (NN) sites in tetrahedral coordination and 12 next-nearest-neighbors (NNN). There are two magnetic rare-earth ions per primitive cell. The lattice and neighbor spacings for both $DyAl_2$ and YAl_2 are listed in Table I, as are a variety of other properties.

The point symmetry of $DyAl_2$ is nearly face-centered cubic, but it lacks inversion symmetry through the origin. This does not affect the expression for the crystalline electric field which can still be written in the cubic form

$$\mathcal{H}_{cf} = B_4(O_4^0 + 5O_4^4) + B_6(O_6^0 - 21O_6^4) , \qquad (16)$$

where the O_j^i are the Stevens operator equivalents. Schelp *et al.*[23] were able to fit the low-temperature heat capacity of $DyAl_2$ from 1.5 to 20 K in external fields up to 7.5 Tesla considering only the crystal field and exchange interactions in a mean-field approximation. The values so obtained for B_4 and B_6 are given in Table I and agree within the quoted error with other measurements, including magnetization of single crystals of $DyAl_2$.[27]

Magnetization measurements have been made by Barbara *et al.*[28] between 4.2 and 180 K. These measurements show that, whereas $GdAl_2$ is an isotropic ferromagnet exhibiting an identical magnetization along the [100] and [111] directions, $DyAl_2$ possesses a strong magnetocrystalline anisotropy with [100] being the easy axis for magnetization. A spin reorientation at 4.2 K was observed along the hard [111] axis in a field of 57 kOe. When extrapolated to zero field, the low-temperature saturation moment along the easy axis was $9.89\mu_B$, close to the free ion value of $10\mu_B$.

B. $(Dy_xY_{1-x})Al_2$ preparation and characterization

The diluted $(Dy_xY_{1-x})Al_2$ compounds ($0.10 \leq x \leq 1.00$) were prepared at the University of Zaragoza. Starting from Dy and Y of 99.9% purity and Al of 99.999% purity, the compounds were repeatedly melted in an argon arc-melting furnace to ensure homogeneity. They were then annealed for one week at a temperature of 800 °C. The polycrystalline samples were cut on a diamond saw into long, rectangular shaped blocks with rough dimensions $1.5 \times 1.5 \times 10$ mm^3. These samples were later cut and shaped with an abrasive to minimize demagnetizing effects. In order to check for the presence of impurity phases, metallographic analyses were performed using both an optical light microscope and scanning electron microscopy (SEM) in the backscattered electron (BSE) mode. A full account of this microanalysis may be found elsewhere.[29,30] No evidence was found for a secondary phase in any of the samples reported in this paper.

Sample concentrations were determined from a wavelength dispersive x-ray analysis of each compound. The results of this study indicate a reasonably uniform concentration profile across the sample surface, which had been significantly smoothed and polished. The maximum difference in x was generally of order 0.01 among five test points. This analysis is typically accurate to no better

TABLE I. Lattice constants and other properties of $DyAl_2$ and YAl_2.

Physical property	$DyAl_2$	YAl_2	Reference
Lattice constant (Å)	7.837±0.003	7.8687±0.0001	20,21
NN spacing (Å)	3.394±0.003	3.4072±0.0001	$\frac{\sqrt{3}}{4}a_0$
NNN spacing (Å)	5.225±0.003	5.2458±0.0001	$\frac{1}{2}a_0$
ρ (gm/cm^3)	5.974±0.002	3.8953±0.0002	(calculated),21
$\mathcal{J}_{NN}$ (THz)	+0.021		22
$\mathcal{J}_{NNN}$ (THz)	+0.010		22
B_4 (10^{-4} meV)	−(0.55±0.13)		23
B_6 (10^{-6} meV)	−(0.556±0.080)		23
E_f (eV)		2.0	(unknown), 24
ϕ_d (eV)	0.08	0.0263	(estimate), 25
K_s(V) (10^{-6}bar^{-1})	0.87±0.02	1.23±0.002	26,21

than 2% of the actual concentration. Nevertheless this is more than adequate for the purposes of this paper.

The $(Dy_xY_{1-x})Al_2$ lattice parameters, determined from x-ray powder diffraction, were found to satisfy Vegard's law. The lattice spacings for the pure compounds were in good agreement with those reported in the literature.[31] This is a strong verification of the dilute, single-phase nature of the $(Dy_xY_{1-x})Al_2$ series.

IV. THE CONTROL PARAMETER $D/\mathcal{J}$

The concept of RMA was first derived to explain the anomalous magnetic behavior of amorphous systems, and so it may appear out of place in a crystalline context.[32] It is important then to list factors that might contribute to the random component of the anisotropy and to estimate their size. Given the strong magnetocrystalline anisotropy in pure $DyAl_2$, it was believed that random substitution of the Dy^{3+} ions with a nonmagnetic, rare-earth counterpart such as Y^{3+} could induce a randomness into the cubic crystal field. Dilution destroys the cubic symmetry of the CEF and should introduce a random uniaxial anisotropy with site-dependent easy axes. Further, since magnetic dilution entails a proportionate reduction in the exchange field, some control should be obtainable over the ratio of the random anisotropy to exchange field strengths $D/\mathcal{J}$, which appears in the AP equation of state [see Eq. (4)].

A. Decrease of $\mathcal{J}$ with dilution

In Fig. 1 the results of high-temperature dc-magnetization measurements, performed in a small calibrated magnetic field, are presented for each of the compounds. The data were fit to a Curie-Weiss law of the form

$$M(T,H) = \chi_b H + \frac{CH}{T-\Theta_p}\ , \tag{17}$$

using a least-squares fitting routine, where χ_b includes both background contributions from the sample holder and the sample Pauli paramagnetism. This was found to be several orders of magnitude smaller than the Curie-Weiss contribution. Demagnetization corrections were made by identifying Θ_p as $\Theta_p - 4\pi NC$, where N is the effective demagnetizating factor along the applied field direction. As only rough estimates could be obtained for the demagnetizing factor for each sample, this quantity is the principal source of error in the determination of Θ_p. Both the Curie constant and the background terms were insensitive to changes in the value of N, as they should be. The result that Θ_p decreases with decreasing x is further evidence of magnetic dilution. In addition, all of the temperatures are positive indicating that the average exchange interaction $\mathcal{J}$ decreases with dilution, but remains positive.

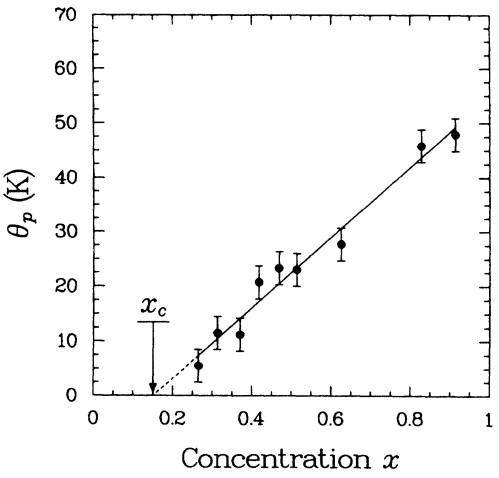

FIG. 1. Dependence of the paramagnetic transition temperature Θ_p on x, the Dy^{3+} concentration. Note that all of the temperatures are positive indicating a positive average exchange interaction $\mathcal{J}$ which decreases with dilution. Extrapolation to $T = 0$ yields an effective percolation threshold of $x_c = 0.15$.

B. Sources of D

Several sources are believed to contribute signficantly to the RMA character of $(Dy_xY_{1-x})Al_2$. Each is discussed at length below and, where possible, an attempt is made to estimate its strength.

1. Distortion of the unit cell

The cubic point symmetry of the unit cell is distorted upon dilution due to the lattice mismatch between $DyAl_2$ and YAl_2. This effect is amplified by the large magnetoelastic coupling in $DyAl_2$.[33] Approximating the elastic constants by the bulk modulus $K_s = 1.1 \times 10^{12}$ erg/cm^3, the magnetoelastic coefficient can be estimated from the saturation magnetostriction $\lambda_t = 1420 \times 10^{-6}$ to be $|B| \approx 1.6 \times 10^9$ erg/cm^3. If the full 0.37% lattice mismatch were to appear as a uniaxial strain, the corresponding change in magnetoelastic energy would correspond to $DJ(J+1) \approx 2.5$ K or $D \approx 0.04$ K. The value of $\mathcal{J}$ from Table I including both $\mathcal{J}_{NN}$ and $\mathcal{J}_{NNN}$ contributions is of order 1.5 K, so that an upper limit of $D/\mathcal{J} \approx 0.027$ can be placed on this source, which is quite weak.

2. Differences in screening

The effective charge screening is different for Y than for Dy, and a simple point charge model for the CEF implies that this difference will lower the local symmetry. The magnitude of this effect will depend in detail on the response of the outer $5d^26s^1$ electrons of the Dy^{3+} ion to a given Dy/Y nearest-neighbor configuration. This contribution is not possible to quantify as there are no

data for the band structure of $DyAl_2$ available in the literature. However, Berthier *et al.*[34] studied NMR data on $(Dy_xY_{1-x})Al_2$ in the concentration range $0.65 \leq x \leq 1.00$, and assumed dilution with Y did not substantially modify the band structure of $DyAl_2$. If this assumption is valid, it is reasonable to conclude that differences in charge screening between Y and Dy will be very slight, which would again argue for a weak RMA strength.

3. *Differences in spin-orbit scattering*

The spin-orbit scattering strength of conduction electrons is different between Y and Dy. Barton and Salamon[35] used this as the primary source of RMA in their early work on *a*-FeMo alloys. They drew on the work of Fert and Levy[36] who demonstrated the presence of a Dzyaloshinky-Moriya type of random off-diagonal exchange interaction due to spin-orbit scattering of conduction electrons by nonmagnetic transition-metal ions. The resulting expression for $D/\mathcal{J}$ is

$$\frac{D}{\mathcal{J}_{\mathrm{RKKY}}} = \frac{15\phi_d}{2E_f}\sin^2\left(\frac{\pi Z_d}{10}\right), \tag{18}$$

where ϕ_d is the difference between the spin-orbit coupling constants of Dy and Y, E_f is the Fermi energy, and Z_d is the number of *d* electrons on the atom providing the differential spin-orbit scattering. The Fermi energy is unavailable for $DyAl_2$, but it should certainly be close to that for YAl_2, which is ≈ 2.0 eV. The spin-orbit coupling constants are tabulated by Griffith[25]; ϕ_d is approximated by the difference between Lu and Y so that $\phi_d \approx 0.08$ eV. Assuming $Z_d = 2$, one obtains $D/\mathcal{J} \leq 0.10$, which is comparable to the lattice-distortion contribution.

Three basic sources of random magnetic anisotropy in $(Dy_xY_{1-x})Al_2$ have been examined. Each serves to lower the local cubic symmetry, the net result of which is to induce a B_2 term into the crystal field Hamiltonian at the expense of higher-order terms. The coefficient of this lowest-order term is the RMA strength D, whose magnitude will contain contributions from all of these effects. While an exact calculation of D is not possible, it is clear that $D/\mathcal{J}$ will be small. Further, the RMA direction will necessarily vary from site to site in a random fashion causing a distribution of local easy axes, the exact number of which will depend on the immediate Dy/Y environment.

The concentration dependence of D is not known analytically, but a maximum in D must be achieved at some intermediate value of the Dy^{3+} concentration. This is reflected in the hysteresis data presented in Fig. 2, where the coercive field H_c and magnetic remanence are plotted as a function of x. A definite maximum is apparent in the neighborhood of 0.70. The small values of H_c (< 400 Oe) are further evidence of weak RMA in these systems and contrast sharply to the tens of kOe found in typical strong RMA systems such as *a*-TbAg.

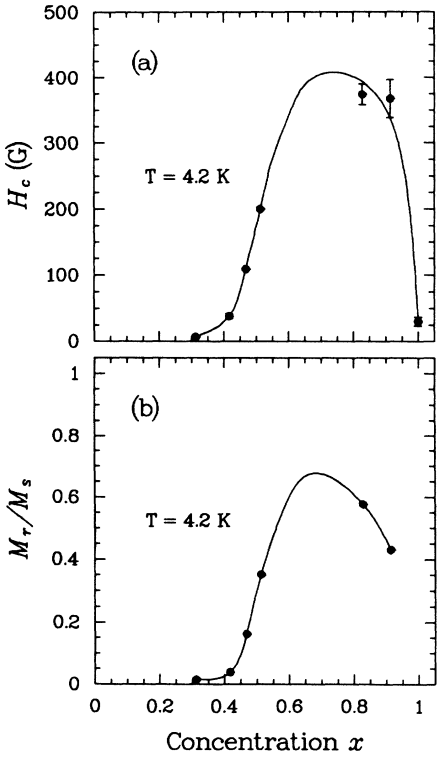

FIG. 2. Coercive and remanent fields versus x. A maximum in the vicinity of x=0.70 is suggestive of a maximum in the RMA strength D. Lines are guides to the eye.

C. Estimate of D from approach to saturation

A more direct method of estimating the RMA strength D exploits the CSS result for the FWA's approach to saturation. Figure 3 shows the fit for the x = 0.370 compound at 5 K using the expression

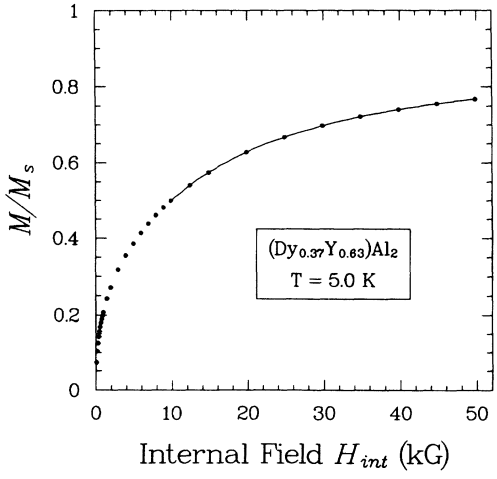

FIG. 3. Fit to the approach of Chudnovsky *et al.* to saturation for x = 0.370.

TABLE II. Parameter values and uncertainties from the fits to the FWA approach to saturation.

x	M_s (G)	H_s (kG)	H_c (kG)	$\chi_b \times 10^{-4}$
0.370	567 ± 20	696 ± 96	1.9 ± 1.1	+1.54 ± 1.5
0.468	716 ± 15	395 ± 48	3.5 ± 0.7	−1.25 ± 1.2
0.513	787 ± 20	292 ± 66	9.1 ± 1.6	−3.14 ± 1.3
0.828	1273 ± 25	169 ± 49	11.0 ± 3.2	+0.83 ± 2.6
0.914	1408 ± 15	131 ± 14	11.5 ± 0.3	−4.11 ± 2.1

$$M(H) = M_s \left[1 - \frac{1}{15}\left(\frac{H_s}{H + H_c}\right)^{1/2}\right] + \chi_b H \ , \qquad (19)$$

where M_s is the saturation magnetization and H_c is the field due to the coherent portion of the anisotropy. This form gave a statistically better fit than did the H^{-2} form of Eq. (15). The fit was performed over a range of fields from 10 to 50 kOe holding M_s fixed at the value

$$M_s = \left(\frac{8x}{a_0^3}\right) 10\mu_B \ , \qquad (20)$$

where a_0 is the lattice spacing, $10\mu_B$ is the Dy^{3+} free-ion moment, and eight is the number of rare-earth ions in the unit cell. For $x = 0.370$, $M_s = 567$ G. Although the fit is excellent, the value obtained for H_s exceeds the maximum field H used in the fit by over a factor of 10. This is true for each of the fits for the other compounds. Thus the condition $H \geq H_s$ is not satisfied. Uncertainties in M_s arise principally from errors in x that are of order 2% and lead to an uncertainty of ±20 G. The corresponding variation in H_s is about 14%. When lower field values are included in the fit, H_s grows larger. Thus the fitted values for H_s are interpreted as upper bounds only.

The root of this problem must lie with the prefactor of $\frac{1}{15}$ in Eq. (19). If this equation were valid only when $H \geq H_s$, the FWA approach to saturation should hold only when the magnetization has reached over 93% of its saturation value. This condition is clearly too general to be true. In light of the good fit achieved for $H \geq 10$ kOe, a prefactor of order unity is indicated.

The values for M_s, H_s, H_c, and χ_b for a number of the samples are listed in Table II. The background term χ_b is always of order 10^{-4} and so never contributes more than 2% to the net magnetization. From Table II it is apparent that H_c increases with x. As the pure limit is approached one expects the amplitude of the coherent anisotropy field to increase. Surprisingly, H_s decreases monotonically with x, never showing a maximum. Note that even if the factor of $\frac{1}{15}$ is adjusted to unity, the random anisotropy field H_s remains comparable to H_c.

The RMA strength can be extracted from the values obtained for H_s. The CSS macroscopic energy density [see Eq. (7)] contains two parameters α and β_r. A simple argument identifies α with the exchange energy through the expression

$$\alpha = \frac{2\mathcal{J}a^2}{\pi^2 \mu M_s} \ . \qquad (21)$$

Similarly, one can argue that β_r is related to D via

$$\beta_r = \frac{2nD}{M_s^2} \ , \qquad (22)$$

where n is the Dy^{3+} spin density. Using this and the expression for α, one obtains the following relation for H_s:

$$H_s = 2\pi^6 \left(\frac{D}{\mathcal{J}}\right)^3 \left(\frac{R_a}{a}\right)^6 \left(\frac{DM_0}{\mu M_s}\right) \ . \qquad (23)$$

An empirical value of $D/\mathcal{J}$ can be obtained by multiplying H_s by T_c^3 and taking the fourth root of the result. This follows from the mean-field result

$$T_c = \left(\frac{2z\mathcal{J}}{3k_B}\right) J(J+1) \ , \qquad (24)$$

which underestimates $\mathcal{J}$, so that the true result should be smaller than that listed in Table III.

Strictly speaking, the values for D and $D/\mathcal{J}$ cannot be compared directly to one another across the concentra-

TABLE III. Table of values for the random anisotropy field strength D/μ_B relative to the exchange field strength H_{ex}, and the ratio $D/\mathcal{J}$. The values for T_c are obtained in the section on scaling.

x	T_c (K)	H_{ex} (kG)	$(D/\mu_B)(R_a/a)^{3/2}$ (kG)	$(D/\mathcal{J})(R_a/a)^{3/2}$
0.914	47.5 ± 0.6	7070 ± 89	2.76 ± 0.11	0.66 ± 0.02
0.828	43.4 ± 0.2	6460 ± 30	2.76 ± 0.25	0.73 ± 0.06
0.513	18.4 ± 0.3	2740 ± 45	1.66 ± 0.14	1.03 ± 0.07
0.468	13.4 ± 0.3	1990 ± 45	1.42 ± 0.07	1.21 ± 0.05
0.370	8.2 ± 0.5	1220 ± 74	1.15 ± 0.11	1.61 ± 0.10

tion series. In part this is because the degree of saturation is not held constant given the limiting field strength of 50 kOe. Higher fields are needed to saturate the magnetization more completely, and would make numerical fits to the perturbative approach of CSS more valid. This is most likely why the RMA strength D increases with decreasing x, rather than achieving the expected maximum value near $x = 0.70$. Furthermore, R_a may depend upon x. These results nonetheless confirm our expectation that the total RMA strength must be weak. The modest assumption of $R_a = 10a$ leads to values of $D/\mathcal{J} \approx 0.05$, well within the range of the estimates made in Sec. IV B.

V. ORDERING IN RMA ALLOYS

A. Low-field magnetic behavior

The thermal dependence of the magnetization M was measured in as low a field as possible for each of the 14 compounds from $0.10 \leq x \leq 1.00$. Such low-field magnetization scans are essential in determining the presence of a "kink" point in the magnetization.[37] Internal demagnetizing fields limit the experimentally measured ratio M/H to a value of $1/4\pi N$, producing a magnetization that is temperature independent below the kink point. This kink point is often considered the *sine qua non* for ferromagnetism.

Each sample was field cooled (FC) from room temperature in the small remanent field of the magnetometer. The field was measured employing an NBS Pd SRM (Standard Reference Material) as a field probe.

The low field magnetization measurements are remarkable in that they show no demagnetizing limited moment for $x \leq 0.828$. Indeed, aside from pure $DyAl_2$, which is known to be ferromagnetic, only the $x = 0.914$ compound exhibits a feature that could be interpreted as a kink point in nominal zero field as shown in Fig. 4. Its magnetization reaches a value of approximately 22 – 23 G as expected for $H = 10.3$ Oe and $N = 0.036$.

The pure compound ($x = 1.00$) is clearly demagnetizing limited. The decrease in magnetization at lower temperatures is attributed to an increase in anisotropy strength that, in this polycrystalline sample, serves to torque a fraction of the spins out of alignment with the applied field. On the other hand, the 0.828 sample is far short of being demagnetizing limited. Its estimated demagnetization factor of $N = 0.014$ produces a demagnetizing limited value of about 21 G in a field of 3.67 Oe, whereas down to $0.23T_c$ the magnetization has not yet exceeded 19 G. Still, no data were obtained below 10 K, and so it is possible that the demagnetizing limit is reached eventually.

It might be argued that dilution alone could cause the observed behavior. Yet if only short-range nearest-neighbor interactions are important, a percolation model predicts that all compounds having $x \geq x_c$ will display LRMO. Because the Dy^{3+} ions sit on diamond lattice sites in the cubic-Laves phase structure, the percolation threshold for the $(Dy_xY_{1-x})Al_2$ system should be 0.428.[38] However, the exchange interaction between Dy^{3+} moments is mediated by the conduction electrons, and the oscillatory nature of the RKKY interaction can raise or lower the effective x_c. In fact, x_c should be lower than the purely nearest-neighbor value of 0.428 since the next nearest-neighbor exchange $\mathcal{J}_{NNN}$ in $DyAl_2$ is also ferromagnetic (see Table I). A ratio of $\mathcal{J}_{NNN}/\mathcal{J}_{NN} = 0.5$ is enough to reduce x_c over 50% in the simple cubic crystal structure.[39] In the case of $(Dy_xY_{1-x})Al_2$, extrapolating the paramagnetic data of Fig. 1 to zero temperature yields an approximate value of $x_c \leq 0.15$. That

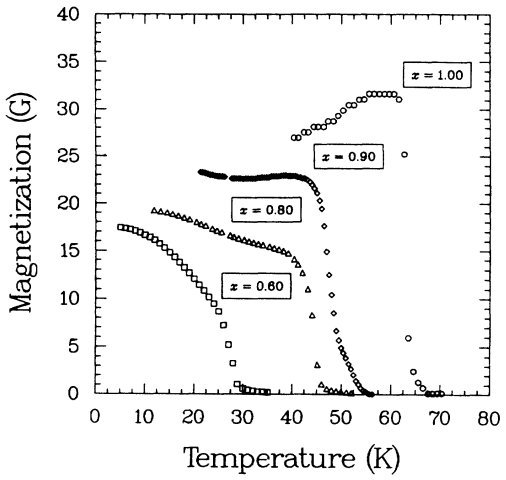

FIG. 4. Magnetization scans for $0.60 \leq x \leq 1.00$. Except for the 0.625 sample, all samples were measured using the VSM magnetometer.

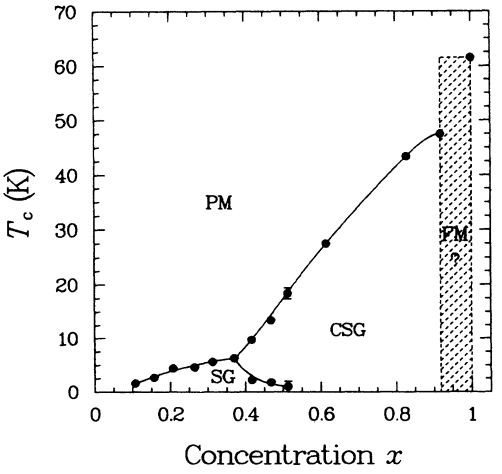

FIG. 5. The designations PM, SG, and CSG stand for the paramagnetic, spin glass, and correlated spin-glass phases, respectively. The hatched area separates the CSG region from that in which ferromagnetic (FM) order may exist.

no spontaneous moment is seen for $x \leq 0.828$ is striking confirmation of the ability of RMA to quench LRMO in $(Dy_xY_{1-x})Al_2$.

The peak positions in the magnetization for the very dilute compounds ($x \leq 0.313$) are plotted versus x in Fig. 5 as are the inflection points that develop for higher concentrations. Also plotted are the peak positions determined from the ac-susceptibility measurements. Together, these data form the basis of a tentative phase diagram in the $H = 0$ plane. These results are discussed in detail in a companion paper.[40]

B. Ferromagneticlike scaling analysis

To explore the validity of a phase transition description for the $(Dy_xY_{1-x})Al_2$ system, a scaling analysis based on equilibrium statistical mechanics was attempted. In this procedure, magnetization data versus temperature and internal field are analyzed employing the usual scaling form of the ferromagnetic equation of state.[41] This is given by

$$\frac{M}{|t|^{\beta}} = f\left(\frac{H}{|t|^{\beta\delta}}\right) , \tag{25}$$

where $f(x)$ is a scaling function, β and δ are critical exponents as described previously, and t is the reduced temperature. The scaling form of Eq. (25) develops two branches, one corresponding to $T < T_c$ and another to $T > T_c$. The uncertainties in the exponents and T_c are estimated by observing the range of values in each quantity that does not disturb the "best" collapsing of the experimental data.

To touch base with a familiar example, the magnetization data for the pure ferromagnetic case of $DyAl_2$ is plotted in Fig. 6. The important feature to notice is the region of the branch for $T < T_c$ where the ordinate becomes nearly independent of the abscissa, marking the development of spontaneous order. At lower temperatures the anisotropy becomes important, and the net moment decreases as **M** attempts to lie along the local easy axis of the polycrystalline sample. The theoretically predicted values for the critical exponents of a 3D Heisenberg system are $\beta = 0.36$ and $\delta = 4.7$. Given the

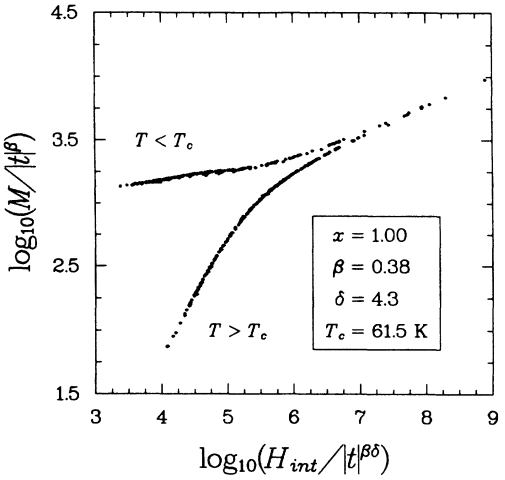

FIG. 6. Scaling plot for $DyAl_2$. A total of 371 data points were used to generate this plot which covers a range of $-0.48 \leq t \leq 0.21$ in reduced temperature and 1 kOe $\leq H \leq$ 3.75 kOe in applied field.

experimentally determined values of $\beta = 0.38 \pm 0.02$ and $\delta = 4.3 \pm 0.3$, the $DyAl_2$ compound can be classified as a three-dimensional Heisenberg ferromagnet with a critical temperature $T_c = 61.5 \pm 0.2$ K, in good agreement with the literature.[22]

This scaling analysis was applied in turn to all compounds from $x = 0.370$ up to the pure limit. Representative plots are shown in Figs. 7 and 8, for $x = 0.828$ and 0.625, respectively. A summary of the scaling results is given in Table IV.

C. Discussion of exponents

Three conclusions can be reached on the basis of the preceding results. First and foremost, for $x < 1$, the branch for $T < T_c$ does not level out in any of the scaling plots; that is, M always depends on H. Instead, each branch appears indicative of a pure power law dependence of M on H. This is in accord with the magnetization temperature profiles presented in Sec. V A, where no

TABLE IV. Critical parameters for the $(Dy_xY_{1-x})Al_2$ system. The exponent γ was obtained using the scaling relation $\gamma = \beta(\delta - 1)$.

x	T_c (K)	β	δ	γ	t range
1.000	61.5 ± 0.5	0.38 ± 0.02	4.3 ± 0.3	1.25 ± 0.2	$-0.48 \leq t \leq 0.21$
0.914	47.5 ± 0.6	1.00 ± 0.20	2.5 ± 0.2	1.50 ± 0.5	$-0.57 \leq t \leq 0.33$
0.828	43.4 ± 0.2	0.61 ± 0.02	2.8 ± 0.2	1.10 ± 0.2	$-0.53 \leq t \leq 0.59$
0.625	27.5 ± 0.1	0.61 ± 0.02	2.9 ± 0.1	1.16 ± 0.1	$-0.09 \leq t \leq 0.13$
0.513	18.4 ± 0.3	0.60 ± 0.03	2.9 ± 0.1	1.14 ± 0.1	$-0.73 \leq t \leq 0.36$
0.468	13.4 ± 0.3	0.60 ± 0.03	2.9 ± 0.1	1.14 ± 0.1	$-0.18 \leq t \leq 0.12$
0.370	8.2 ± 0.5	0.75 ± 0.05	2.5 ± 0.1	1.15 ± 0.2	$-0.39 \leq t \leq 3.27$

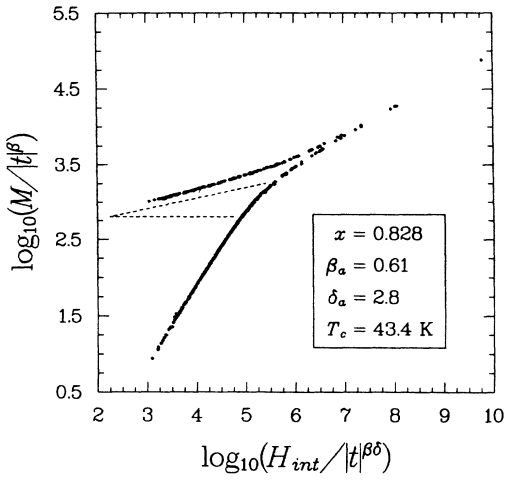

FIG. 7. Scaling plot for $x = 0.828$. The plot spans $-0.53 \leq t \leq 0.59$ in reduced temperature and 500 Oe $\leq H \leq$ 1.4 kOe in applied field. A total of 396 points were used to generate the plot.

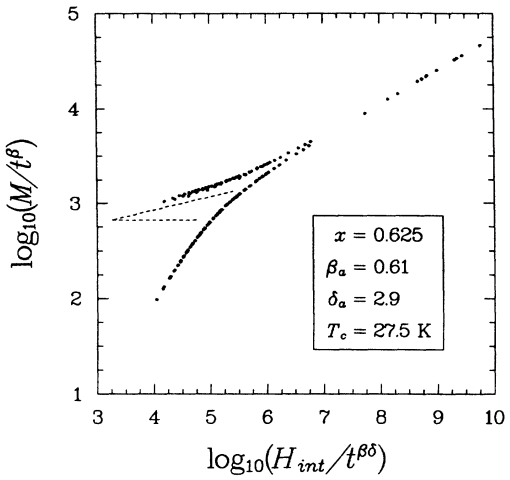

FIG. 8. Scaling plot for $x = 0.625$. The plot spans $-0.09 \leq t \leq 0.13$ in reduced temperature and 300 Oe $\leq H \leq$ 5.0 kOe in applied field. A total of 155 points were used to generate the plot.

sample exhibited a demagnetizing limited magnetization in nominal zero field, except possibly for $x = 0.914$.

That the data scale so well provides a strong indication that a true thermodynamically driven phase transition occurs in the $(Dy_xY_{1-x})Al_2$ system, and lends credence to the tentative assignment made in Sec. V A of a critical line of transitions separating the PM phase from the CSG phase in the phase diagram. Further, data taken over a wide range of fields and temperatures obey the scaling relation. It is an unanswered question as to why scaling theory works as well as it does so far from the critical regime. However, one must bear in mind that no spontaneous moment ever develops, and so the magnetization M cannot be viewed as the proper order parameter for these compounds.

The actual values of the exponents are noteworthy. Except for $x \geq 0.914$, the values for δ lie near 2.9, and those for β lie near 0.60. This uniformity of scaling is striking indeed and suggests that some crossover has taken place from pure $d = 3$ Heisenberg exponents to those describing random magnetic anisotropy. These values cannot be classified with any known universality class such as those represented by the three-dimensional Heisenberg, XY, or Ising ferromagnets. Even an assumption of some sort of dimensionality reduction resulting from dilution does not work since the values of the exponents lie far from the two-dimensional Ising values of $\beta = 0.25$ and $\delta = 15$. Since there is no spontaneous moment in these compounds, within experimental uncertainty, the critical exponent β can no longer have the meaning it enjoyed in the ferromagnetic case where it governed the thermal dependence of the spontaneous magnetization. The question naturely arises, then, of the precise meaning of these RMA exponents.

By modifying the AP (Ref. 2) RMA equation of state, one can establish a direct connection between the RMA exponents and those describing the pure ferromagnetic compound $DyAl_2$. Starting with Eq. (4), one replaces (H/M) with $(H/M)^{1/\gamma}$ and M^2 with $M^{1/\beta}$ as is done for the so-called modified Arrott plots. Thus, one has

$$\left(\frac{H}{M}\right)^{1/\gamma} = t + M^{1/\beta} + a_A \left(\frac{n-1}{n(n+2)}\right)\left(\frac{D}{\mathcal{J}}\right)^2 M^{1/\beta}\left(\frac{H}{M}\right)^{-\epsilon/2\gamma}, \tag{26}$$

where $\epsilon = 4-d$ as before. One then examines two limiting cases. Near T_c, both t and $M^{1/\beta}$ are small so that

$$H \sim M^{1+2\gamma/(\epsilon+2)\beta}, \tag{27}$$

from which one identifies the RMA exponent

$$\delta_a = 1 + \frac{2\gamma}{(\epsilon+2)\beta}, \tag{28}$$

Note that in $d = 4$ dimensions

$$\delta_a = 1 + \frac{\gamma}{\beta} = \delta \tag{29}$$

since $\epsilon = 0$. At very low temperature, the inverse susceptibility (H/M) approaches zero as $H \to 0$ so that

$$H \sim |t|^{-2\gamma/\epsilon} M^{1+2\gamma/\epsilon\beta}. \tag{30}$$

Thus,

$$\delta_1 = 1 + \frac{2\gamma}{\epsilon\beta} \tag{31}$$

by definition of δ_1. Here $\delta_1 \to \infty$ for $\epsilon = 0$, which simply means M has lost its dependence on H, i.e., ferromagnetism is restored in four dimensions. One can easily recover the AP values of $\delta_a = \frac{7}{3}$ and $\delta_1 = 5$ in the limit that $\beta = \frac{1}{2}$ and $\gamma = 1$ for $d = 3$. The ferromagnetic scaling form given by Eq. (25) is now rewritten in the form

$$M/t^{\beta_a} = f(H/t^{\beta_a\delta_a}) \equiv f(x) \to x^{1/\delta_1} , \tag{32}$$

in the limit of low temperatures, $T < T_c$. Here β_a and δ_a are subscripted to distinguish them from the "pure" critical exponents. Then,

$$H \sim |t|^{-\beta_a(\delta_1-\delta_a)} M^{\delta_1} . \tag{33}$$

Equating exponents of $|t|$ in this equation and Eq. (30) and substituting in the known expressions for δ_1 and δ_a yields the following relation between the RMA exponent β_a and β:

$$\beta_a = \left(\frac{\epsilon+2}{2}\right)\beta = \left(\frac{6-d}{2}\right)\beta . \tag{34}$$

Since $d = 3$, the theoretical value for β_a is $\frac{3}{2}$ times the pure value for β, which is 0.38 ± 0.02, i.e.,

$$\beta_a = 0.57 \pm 0.03 . \tag{35}$$

This value agrees remarkably well with the experimental values of 0.60 and 0.61 obtained from the scaling analysis of the magnetization data for $0.40 \leq x \leq 0.80$. (Note that the mean-field value for β_a is 0.75.) At the same time,

$$\delta_a = 3.00 \pm 0.13 , \tag{36}$$

which is entirely consistent with the experimental values of 2.9 to 2.8.

Although the scaling analysis does not yield values for δ_1 directly, these can be estimated from the slope of the subcritical branch at the lowest temperatures. The preceding analysis predicts

$$\delta_1 = 7.00 \pm 0.39 . \tag{37}$$

This exceeds the experimental values, determined from the low temperature slopes of the subcritical branch of the scaling plots, which range from 4.7 to 5.3 over the same concentration range. In all probability the data do not reach the asymptotic limit. To illustrate this point graphically, a line with slope $1/\delta_1$ ($\frac{1}{7}$) has been drawn on the two scaling plots in Figs. 7 and 8.

It is important to point out that the modified AP equation of state has a form almost identical to that derived by GA (Ref. 7) to leading order in the random anisotropy, and in the limit of zero uniform anisotropy and random fields. The sole difference is that the exponent $\epsilon/2\gamma$ in Eq. (26) is just $\epsilon/2$, i.e., there is no γ in the denominator. However, should it be the case that the crossover exponent $\phi_a = \epsilon/2 = 0.5$ for $N = 3$ and $d = 3$, the two equations of state would agree. In view of the fact that the AP equation of state is only valid in the limit of vanishing $D/\mathcal{J}$, it is quite remarkable that this modification can account for the observed scaling behavior so well.

D. Limits on χ: $(\mathcal{J}/D)^4$ or $(4\pi N)^{-1}$?

A few comments concerning the size of χ are in order. The pure compound clearly has a demagnetizing limited susceptibility. However, neither the 0.914 nor the 0.828 compound susceptibility reach their respective demagnetizing limits. In fact, χ never exceeds 40% of $1/4\pi N$ in either case. However, there is a striking difference in both the field and temperature dependences of the susceptibility between the 0.914 and 0.828 compounds. For $x = 0.914$, χ exhibits a maximum as a function of field. Moreover, this peak position is temperature dependent, as is its size, the maximum occuring at T_c. In contrast, the susceptibility for $x = 0.828$ increases monotonically both with decreasing temperature and field down to as low as 10 Oe. At present, more data is needed to characterize fully the temperature and field dependences of χ for all concentrations.

Because the ratio $D/\mathcal{J}$ has only been determined to within the unknown factor R_a/a, it is not possible to compare quantitatively the measured susceptibilities with the theoretical form $(\mathcal{J}/D)^4$ for each compound. The work of Barbara *et al.*[16] has shown, in any case, that weak RMA systems ($D/\mathcal{J} < 0.3$) can deviate substantially from this form. The one firm conclusion that can be reached is that no sample exhibits a demagnetizing limited susceptibility, but that below $x = 0.914$, χ increases dramatically at low fields and low temperatures. At lower temperatures and fields some limiting value must be attained. Whether it is intrinsically limited by the RMA or by demagnetizing fields remains an issue to be resolved in a future study.

VI. CONCLUSIONS

Until now, $(Dy_xY_{1-x})Al_2$ has been believed to be ferromagnetic over most of the concentration range. However, the results of this paper show that LRMO in pure $DyAl_2$ is destroyed by as little as 10% dilution with nonmagnetic Y, far above the percolation threshold. This is seen to be a consequence of the dilution-induced randomness in the magnetocrystalline anisotropy of $DyAl_2$, whose effects have been modeled, with varying degrees of success, by the weak RMA theories of Aharony and Pytte [2] and Chudnovsky *et al.*[3]

In addition to underscoring the fragile nature of LRMO in the presence of weak RMA, the results presented here have shown that a random component can be introduced into the magnetocrystalline anisotropy by site dilution of a crystalline material without having to resort to the use of amorphous materials. When the dilution proceeds

by the introduction of nonmagnetic impurities, the corresponding reduction in the exchange interaction $\mathcal{J}$ combines with D to give a range of effective RMA strengths. Modulo the unknown factor of R_a/a, $D/\mathcal{J}$ ranges from 0.66 to 1.6 as x decreases from 0.914 to 0.370. These numbers corroborate the estimates made in Sec. III which were of order 0.1 or less. This requires R_a to be only a few lattice spacings, an entirely reasonable value. However, more work is needed to clarify what happens at lower concentrations and higher fields.

A dramatic increase in the bulk magnetization is observed in passing from the high-temperature paramagnetic phase to temperatures $T \leq T_c$ for $x \geq 0.370$. To test the relevance of a phase transition description for this line of transitions, a scaling analysis pertinent to ferromagnets was applied. Remarkably, excellent scaling fits are obtained for each compound, with critical exponents that are independent of x over a wide range of concentration. As no spontaneous moment is seen in any of these compounds (with the possible exception of the $x = 0.914$ compound), this low-temperature phase cannot be ferromagnetic. Nevertheless, these results strongly suggest the existence of a true thermodynamically driven phase transition to a novel magnetic state. Moreover, the critical exponents cannot be reconciled with any known universality class, even assuming the possibility of a dimensionality reduction due to the dilution. Instead, by modifying the AP equation of state, agreement between theory and experiment is achieved, lending further credence to the claim that a novel low-temperature phase replaces LRMO in the presence of weak RMA.

Goldschmidt and Aharony[7] argue that this phase is a spin-glass phase in the absence of any uniform anisotropy (cubic, hexagonal, etc.), but that if sufficiently strong, these anisotropies can stablize the ferromagnetic state. On the other hand, Fisher[17] has argued on theoretical grounds that the proof of a spin-glass or ferromagneticlike phase in the presence of RMA is still an open question. Clearly, more work is necessary on both theoretical and experimental sides in order to elucidate fully the nature of this RMA-induced phase.

ACKNOWLEDGMENTS

Thanks are due to Dr. Ian Steele of the University of Chicago Electron Microprobe Lab for sample analysis, as well as to Cameron Begg and John Woodhouse of the University of Illinois for their assistance. This research was supported by the National Science Foundation under Grant No. NSF DMR 86-12860.

---

*Present address: Physics Department, Brookhaven National Laboratory, Upton, NY 11973.

[1] T. C. Lubensky, Phys. Rev. B **11**, 3573 (1975).
[2] A. Aharony and E. Pytte, Phys. Rev. Lett. **45**, 1583 (1980).
[3] E. M. Chudnovsky, W. M. Saslow, and R. A. Serota, Phys. Rev. B **33**, 251 (1986).
[4] R. Harris, M. Plischke, and M. J. Zuckermann, Phys. Rev. Lett. **31**, 160 (1973).
[5] Y. Imry and S.-K. Ma, Phys. Rev. Lett. **21**, 1399 (1975).
[6] A. Aharony and E. Pytte, Phys. Rev. B **27**, 5872 (1983).
[7] Y. Y. Goldschmidt and A. Aharony, Phys. Rev. B **32**, 264 (1985).
[8] J. J. Rhyne, S. J. Pickart, and H. A. Alperin, Phys. Rev. Lett. **29**, 1562 (1972).
[9] R. J. Elliott, *Magnetic Properties of Rare Earth Metals* (Plenum, New York, 1972).
[10] R. W. Cochrane, R. Harris, and M. J. Zuckermann, Phys. Rep. **48**, 3 (1978).
[11] R. Ferrer, R. Harris, D. Zobin, and M. J. Zuckermann, Solid State Commun. **26**, 451 (1978); J. Filippi, B. Dieny, and B. Barbara, Solid State Commun. **53**, 523 (1985).
[12] B. Boucher, Phys. Status Solidi (a) **40**, 197 (1977).
[13] J. A. Gerber, S. G. Cornelison, W. L. Burmester, and D. J. Sellmyer, J. Appl. Phys. **50**, 1608 (1979).
[14] R. A. Pelcovits, E. Pytte, and J. Rudnick, Phys. Rev. Lett. **40**, 476 (1978).
[15] S. von Molnar, T. R. McGuire, R. J. Gambino, and B. Barbara, J. Appl. Phys. **53**, 7666 (1982).
[16] B. Barbara, M. Couach, and B. Dieny, Europhys. Lett. **3**, 1129 (1987).
[17] D. Fisher, Phys. Rev. B **31**, 7233 (1985).
[18] D. J. Sellmyer and S. Nafis, J. Appl. Phys. **57**, 3584 (1985).
[19] S. M. Jaakkola and M. K. Hänninen, Solid State Commun. **36**, 275 (1980).
[20] J. H. Wernick and S. Geller, Trans. AIME **218**, 866 (1960).
[21] R. J. Schiltz Jr. and J. F. Smith, J. Appl. Phys. **45**, 4681 (1974).
[22] T. M. Holden, W. J. L. Buyers, and H.-G. Purwins, J. Phys. F **14**, 2701, (1984).
[23] W. Schelp, W. Drewes, A. Leson, and H.-G. Purwins, J. Phys. Chem. Solids **47**, 855 (1986).
[24] A. Hasegawa and A. Yanase, J. Phys. F **10**, 2207 (1980).
[25] J. S. Griffith, *The Theory of Transition Metal Ions* (Cambridge University Press, Cambridge, England, 1961), pp. 113 and 468.
[26] G. Dublon, H. Klimker, U. Atzmony, M. P. Dariel, M. Rosen, A. Grayewski, and D. Fekete, Phys. Lett. **53A**, 23 (1975).
[27] D. Kohake, A. Leson, H.-G. Purwins, and A. Furrer, Solid State Commun. **43**, 965 (1982).
[28] B. Barbara, M. F. Rossignol, H.-G. Purwins, and E. Walker, in *Crystal Field Effects in Metals and Alloys*, edited by A. Furrer (Plenum, New York, 1977), pp. 148 – 152.
[29] J. I. Arnaudas, Ph. D. thesis, University of Zaragoza, 1985.
[30] P. M. Gehring, Ph. D. thesis, University of Illinois, 1989.
[31] K. H. J. Buschow, Rep. Prog. Phys. **42**, 1373 (1979).
[32] See, however, K. Siratori, K. Kohn, H. Suwa, E. Kita, S. Tamura, F. Sakai, and A. Tasaki, J. Phys. Soc. Jpn. **51**, 2746 (1982); A. J. Dirkmaat, D. Hüser, G. J. Nieuwenhuys, J. A. Mydosh, P. Kettler, and M. Steiner, Phys. Rev. B **36**, 352 (1987).
[33] F. Pourarian and W. E. Wallace, J. Appl. Phys. **50**, 7707 (1979).

[34]Y. Berthier, R. A. B. Devine, and B. Barbara, Phys. Rev. B **16**, 1025 (1977).
[35]L. S. Barton and M. B. Salamon, Phys. Rev. B **25**, 2030 (1982).
[36]A. Fert and P. M. Levy, Phys. Rev. Lett. **44**, 1538 (1980); P. M. Levy and A. Fert, Phys. Rev. B **23**, 4667 (1981).
[37]P. J. Wojtowicz and M. Rayl, Phys. Rev. Lett. **20**, 1489 (1968).
[38]D. Stauffer, Phys. Rep. **54**, 1 (1979).
[39]H. Dvey-Aharon and M. Fibich, Phys. Rev. B **18**, 3491 (1978).
[40]A. del Moral, P. M. Gehring, J. I. Arnaudas, and M. B. Salamon (unpublished).
[41]P. Pfeuty and G. Toulouse, *Introduction to the Renormalization Group and Critical Phenomena* (Wiley, New York, 1977), p. 53.